Effect of Carbon Doping on the Structure and Magnetic Phase Transition in (Mn,Fe$_2$(P,Si))

Nguyên, V.T.; Yibole, H.; Miao, X. F.; Goubitz, K.; van Eijck, L.; van Dijk, N.H.; Brück, E.

Important note
To cite this publication, please use the final published version (if applicable).
Please check the document version above.

CrossMark

Effect of Carbon Doping on the Structure and Magnetic Phase Transition in (Mn,Fe₂(P,Si))

N.V. THANG,[1,3] H. YIBOLE,[1] X.F. MIAO,[1] K. GOUBITZ,[1] L.VAN EIJCK,[2] N.H.VAN DIJK,[1] and E. BRÜCK[1]

1.—Fundamental Aspects of Materials and Energy, Department of Radiation Science and Technology, Delft University of Technology, Mekelweg 15, 2629 JB Delft, The Netherlands. 2.—Neutron and Positron Methods in Materials, Department of Radiation Science and Technology, Delft University of Technology, Mekelweg 15, 2629 JB Delft, The Netherlands. 3.—e-mail: v.t.nguyen-1@tudelft.nl

Given the potential applications of (Mn,Fe₂(P,Si))-based materials for room-temperature magnetic refrigeration, several research groups have carried out fundamental studies aimed at understanding the role of the magneto-elastic coupling in the first-order magnetic transition and further optimizing this system. Inspired by the beneficial effect of the addition of boron on the magnetocaloric effect of (Mn,Fe₂(P,Si))-based materials, we have investigated the effect of carbon (C) addition on the structural properties and the magnetic phase transition of $Mn_{1.25}Fe_{0.70}P_{0.50}Si_{0.50}C_z$ and $Mn_{1.25}Fe_{0.70}P_{0.55}Si_{0.45}C_z$ compounds by x-ray diffraction, neutron diffraction and magnetic measurements in order to find an additional control parameter to further optimize the performance of these materials. All samples crystallize in the hexagonal Fe₂P-type structure (space group P-62m), suggesting that C doping does not affect the phase formation. It is found that the Curie temperature increases, while the thermal hysteresis and the isothermal magnetic entropy change decrease by adding carbon. Room-temperature neutron diffraction experiments on $Mn_{1.25}Fe_{0.70}P_{0.55}Si_{0.45}C_z$ compounds reveal that the added C substitutes P/Si on the 2c site and/or occupies the 6k interstitial site of the hexagonal Fe₂P-type structure.

INTRODUCTION

Room-temperature magnetic refrigeration exploiting the magnetocaloric effect (MCE) of magnetic materials has the potential to address the disadvantages of conventional vapor-compression refrigeration when it comes to the environmental impact, energy efficiency and device volume.[1–3] Magnetic marterials showing large low-field magnetocaloric effect have been attracting increasing attention over the past few decades due to their potential applications for magnetic refrigeration. During the past decades, a large MCE in the room-temperature range has been observed in several classes of materials including $Gd_5(Si,Ge)_4$;[4] MnAs and Mn(As,Sb);[5,6] $(Mn,Fe)_2(P,X)$ with X = As, Ge, Si;[7–9] $(Mn,Fe)_2(P,Si,B)$;[10] $MnCoGeB_x$;[11] $MnCoGe_{1-x}Ga_x$;[12] $MnCo_{1-x}Fe_xSi$;[13] $La(Fe,Si)_{13}$ and their hydrides;[14,15] $La(Mn,Fe,Si)_{13}H_z$;[16] $Fe_{49}Rh_{51}$[17] and Heusler alloys.[18,19] A combination of a large MCE, tuneable Curie temperature, limited thermal hysteresis, non-toxic and abundant ingredients makes $(Mn,Fe)_2(P,Si)$-based compounds one of the most attractive candidate materials for commercial room-temperature magnetic refrigeration.

In order to cover a wide range of temperatures, different magnetocaloric materials with the desired variation in T_C are required, while having both a large MCE and a small thermal hysteresis. With the aim to tune the Curie temperature and reduce the thermal hysteresis, while improving the mechanical stability and maintaining an acceptable MCE in the $(Mn,Fe)_2(P,Si)$ system, much work has recently been done by balancing the Mn:Fe ratio and P:Si ratios,[20,21] by the introduction of nitrogen,[22,23] by varying the duration and temperature of the heat treatment[24] and by Co-B and Ni-B co-doping.[25] Miao et al. (Ref. 23) have recently shown that the magnetic

transition of $(Mn,Fe)_2(P,Si)$ can be tailored by adding C. The C atoms were found to occupy the interstitial $6k$ and $6j$ sites in the hexagonal structure. The aim of the present study is to obtain the complementary information on the influence of C additions on the magnetocaloric properties, which is key information that needs to be taken into account for practical
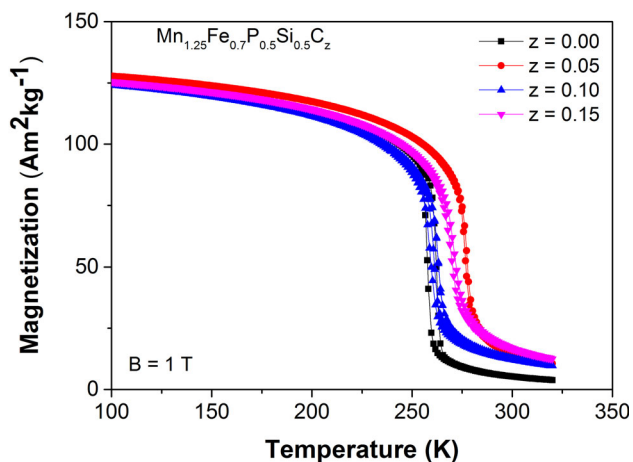
applications. Based on the earlier studies by Miao et al. (Ref. 23) the C atoms were expected to be introduced interstitially, and; therefore, the C was added to the composition (rather than substituted for another element).

To study the influence of C on the structural and magnetocaloric properties of $(Mn,Fe)_2(P,Si)$-based materials, in this work, C was added to the $Mn_{1.25}Fe_{0.70}P_{0.50}Si_{0.50}$ and $Mn_{1.25}Fe_{0.70}P_{0.55}Si_{0.45}$ compounds. These two compounds have been chosen for this work due to their different magnitude of latent heat. In fact, an increase in P/Si ratio leads to a stronger first-order magnetic transition. The influence of carbon addition on the structural, magnetic and magnetocaloric properties of the compounds obtained was systematically investigated by x-ray diffraction and magnetic measurements. In order to determine the occupancy of C added in the crystal structure, room-temperature neutron diffraction was employed for $Mn_{1.25}Fe_{0.70}P_{0.55}Si_{0.45}C_z$ compounds. This may allow understanding the relation between the changes in crystal structure and in the magnetic phase transition.

Fig. 1. Magnetization of the $Mn_{1.25}Fe_{0.70}P_{0.50}Si_{0.50}C_z$ compounds as a function of temperature during heating and cooling at a rate of 2 K/min in a magnetic field of 1 T.

EXPERIMENTAL

To investigate the influence of carbon addition on the structural properties and magnetic phase transition, two series of samples, $Mn_{1.25}Fe_{0.70}P_{0.50}Si_{0.50}C_z$

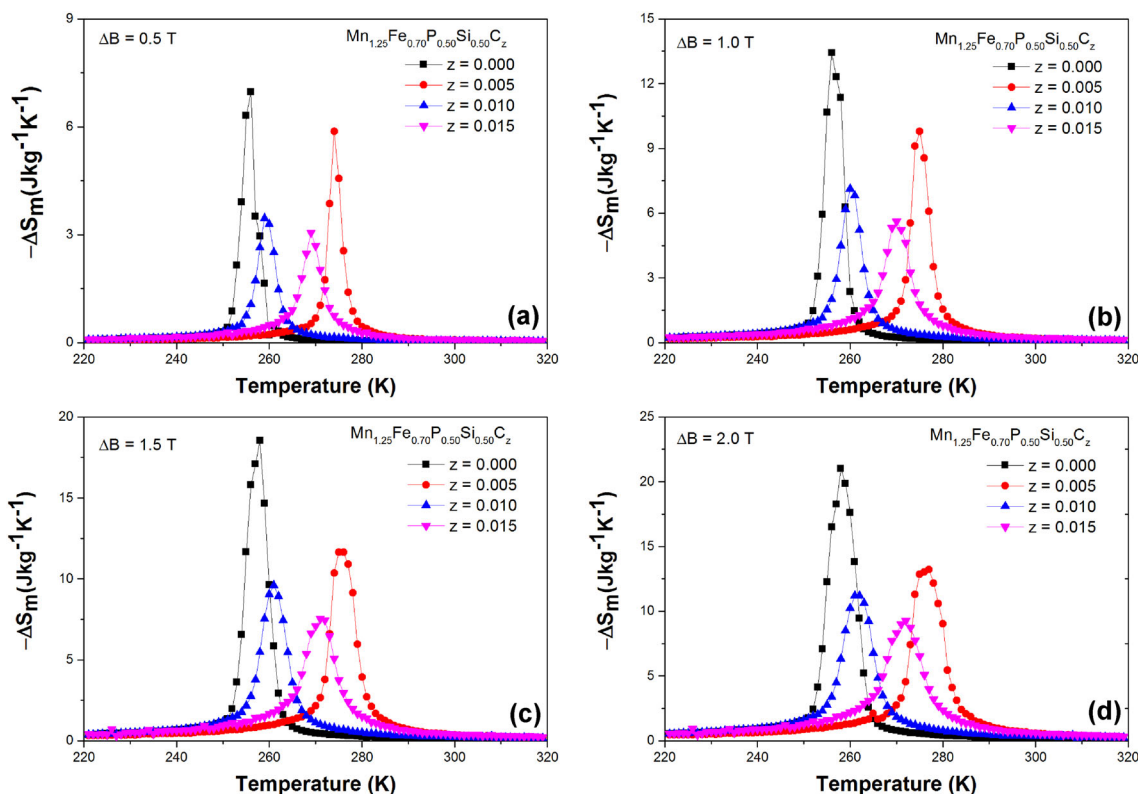Fig. 2. Isothermal magnetic entropy change of the $Mn_{1.25}Fe_{0.70}P_{0.50}Si_{0.50}C_z$ compounds as a function of temperature for a field change of 0.5 (a), 1.0 (b), 1.5 (c) and 2.0 T (d).

and $Mn_{1.25}Fe_{0.70}P_{0.55}Si_{0.45}C_z$, were prepared by high-energy ball milling followed by a double-step annealing process.[26] The mixtures of 15 g starting materials, namely Fe, Mn, red-P, Si and C (graphite), were ball milled for 16.5 h (having a break for 10 min every 15-min milling) with a constant rotation speed of 380 rpm in tungsten-carbide jars with seven tungsten-carbide balls under argon atmosphere. The fine powders obtained were compacted into small tablets and were then sealed into quartz ampoules with 200 mbar argon before the heat treatment was performed.

Magnetic properties were characterized using a commercial superconducting quantum interference device (SQUID) magnetometer (Quantum Design MPMS XL) in the reciprocating sample option (RSO) mode. X-ray powder diffraction experiments using a PANalytical X-pert Pro diffractometer with Cu-K$_\alpha$ radiation were carried out at room temperature. The room temperature neutron diffraction data were collected on the neutron powder diffraction instrument PEARL[27] at the research reactor of Delft University of Technology. For neutron measurements, 8–10 g powder samples were put into a vanadium can with a diameter of 6 mm and a height of 50 mm. Structure refinement of the x-ray and neutron diffraction data was done by using the Rietveld method implemented in the Fullprof program.[28]

RESULTS AND DISCUSSION

$Mn_{1.25}Fe_{0.70}P_{0.50}Si_{0.50}C_z$ Compounds

The room temperature XRD patterns of the $Mn_{1.25}Fe_{0.70}P_{0.50}Si_{0.50}C_z$ ($z = 0.00$, 0.05, 0.10 and 0.15) compounds indicate that all samples exhibit the hexagonal Fe_2P-type main phase. The temperature dependence of the magnetization for the $Mn_{1.25}Fe_{0.70}P_{0.50}Si_{0.50}C_z$ compounds was measured during cooling and heating after removing the 'virgin effect'[29] under an applied magnetic field of 1 T and is shown in Fig. 1. All samples show sharp ferro-to-paramagnetic phase transitions accompanied by a small thermal hysteresis. The Curie temperature (T_C) increases while the thermal hysteresis (ΔT_{hys}) decreases as carbon is added.

However, the change in T_C is not linear as a function of the carbon content. Compared to B doping,[30] the influence of C doping on both T_C and ΔT_{hys} is less pronounced.

The isothermal entropy change (ΔS_m) of the $Mn_{1.25}Fe_{0.70}P_{0.50}Si_{0.50}C_z$ compounds in a field change of 0.5 T, 1.0 T, 1.5 T and 2.0 T derived from the isofield magnetization curves for cooling using the Maxwell relation is shown in Fig. 2 and summarized in Table I. It is noticeable that for magnetic field changes of between 0.5 T and 2.0 T, ΔS_m decreases as a function of carbon concentration although T_C does not show a systematic change for increasing carbon concentration. Moreover, the $Mn_{1.25}Fe_{0.70}P_{0.50}Si_{0.50}C_{0.05}$ compound shows nice magnetocaloric properties in low field (0.5 T) accompanied by a very small (negligible) thermal hysteresis. An acceptable magnetocaloric effect at lower magnetic field strength would be a significant advantage for practical applications, since it allows reducing the mass of permanent magnets needed to generate the magnetic field. Thus, it is highly desirable to verify the effect of carbon doping on
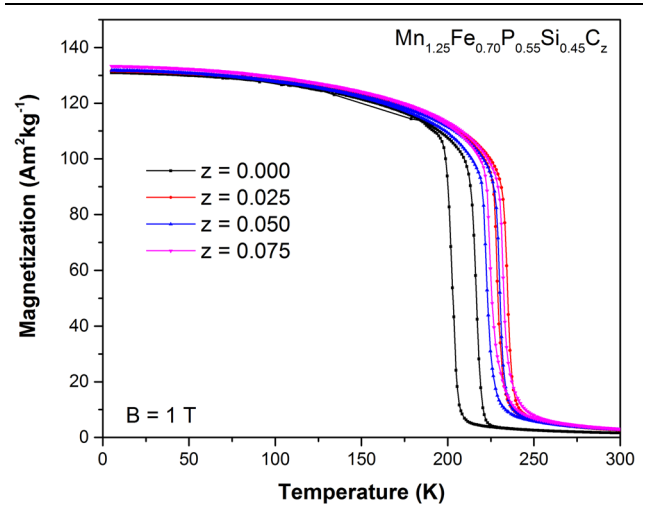
Fig. 3. Magnetization of $Mn_{1.25}Fe_{0.70}P_{0.55}Si_{0.45}C_z$ compounds as a function of temperature during heating and cooling at a rate of 2 K/min in a magnetic field of 1 T.

Table I. Curie temperature (T_C) derived from the magnetization curves measured on cooling, the isothermal entropy change (ΔS_m) derived from the isofield magnetization curves in a field change of 0.5 T, 1.0 T, 1.5 T and 2.0 T, thermal hysteresis (ΔT_{hys}) derived from the magnetization curves measured in 1 T upon cooling and heating for the $Mn_{1.25}Fe_{0.70}P_{0.50}Si_{0.50}C_z$ compounds

		$\Delta S_m(JK^{-1}kg^{-1})$				
z	T_C (K)	$\Delta B = 0.5$ T	$\Delta B = 1.0$ T	$\Delta B = 1.5$ T	$\Delta B = 2.0$ T	ΔT_{hys} (K)
0.00	256	6.97	14.43	18.56	21.01	4.6
0.05	275	5.88	9.79	11.65	13.02	0.5
0.10	260	3.46	7.12	9.60	11.19	3.5
0.15	270	3.05	5.61	7.53	9.21	1.3
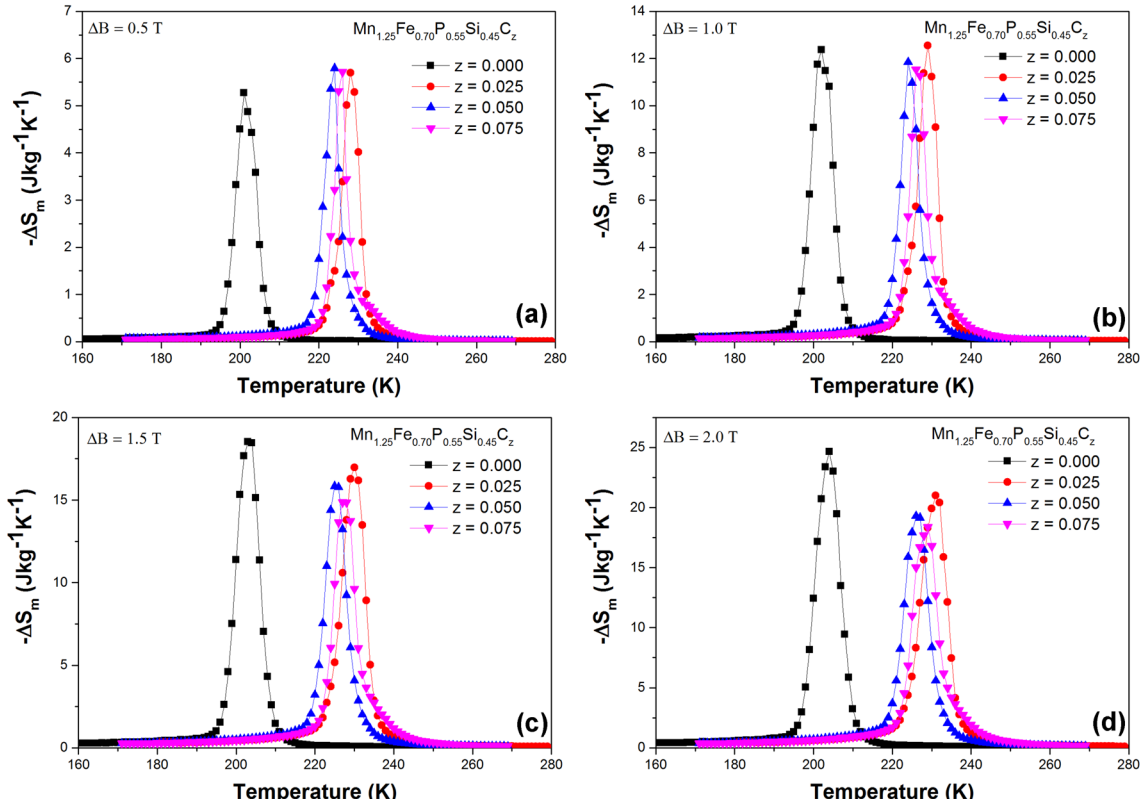
Fig. 4. Isothermal magnetic entropy change of the Mn$_{1.25}$Fe$_{0.70}$P$_{0.55}$Si$_{0.45}$C$_z$ compounds as a function of temperature for a field change of 0.5 (a), 1.0 (b), 1.5 (c) and 2 T (d).

Table II. Curie temperature (T_C) derived from the magnetization curves measured on cooling, the isothermal entropy change (ΔS_m) derived from the isofield magnetization curves in a field change of 0.5 T, 1.0 T, 1.5 T and 2.0 T, thermal hysteresis (ΔT_{hys}) derived from the magnetization curves measured in 1 T upon cooling and heating for the Mn$_{1.25}$Fe$_{0.70}$P$_{0.55}$Si$_{0.45}$C$_z$ compounds

		ΔS_m (JK^{-1}kg^{-1})				
z	T_C (K)	$\Delta B = 0.5$ T	$\Delta B = 1.0$ T	$\Delta B = 1.5$ T	$\Delta B = 2.0$ T	ΔT_{hys} (K)
0.000	202	5.27	12.36	18.53	24.64	13.4
0.025	229	5.70	12.55	16.98	20.99	5.4
0.050	224	5.79	11.83	15.82	19.28	7.4
0.075	226	5.71	11.53	14.86	18.38	7.3

the thermal hysteresis, magnetic phase transition and magnetocaloric properties of (Mn,Fe)$_2$(P,Si)-based compounds.

Mn$_{1.25}$Fe$_{0.70}$P$_{0.50}$Si$_{0.45}$C$_z$ Compounds

To verify the influence of carbon added on the magnetic phase transition and the thermal hysteresis of (Mn,Fe)$_2$(P,Si)-based compounds, another series of samples with the parent compound was prepared. Room-temperature XRD patterns of Mn$_{1.25}$Fe$_{0.70}$P$_{0.55}$Si$_{0.45}$C$_z$ compounds indicate that the hexagonal Fe$_2$P-type structure remains unchanged by adding C. This confirms that the carbon addition preserved the crystal structure of (Mn,Fe)$_2$(P,Si).

Figure 3 shows the temperature dependence of the magnetization for the Mn$_{1.25}$Fe$_{0.70}$P$_{0.55}$Si$_{0.45}$C$_z$ compounds. A remarkable thermal hysteresis confirms that the nature of the phase transitions in the parent and doped compounds is of the first order. It is noticeable that the Curie temperature can be tuned between 202 K and 226 K, while maintaining the sharp magnetic phase transition and reducing the thermal hysteresis by the introduction of carbon

Table III. The C concentrations in $Mn_{1.25}Fe_{0.70}P_{0.55}Si_{0.45}C_z$ compounds

Nominal composition	Nominal wt.% C	Measured wt.% C
$Mn_{1.25}Fe_{0.70}P_{0.55}Si_{0.45}$	0.00	0.06 (5)
$Mn_{1.25}Fe_{0.70}P_{0.55}Si_{0.45}C_{0.025}$	0.22	0.24 (5)
$Mn_{1.25}Fe_{0.70}P_{0.55}Si_{0.45}C_{0.050}$	0.43	0.43 (5)
$Mn_{1.25}Fe_{0.70}P_{0.55}Si_{0.45}C_{0.075}$	0.65	0.64 (5)

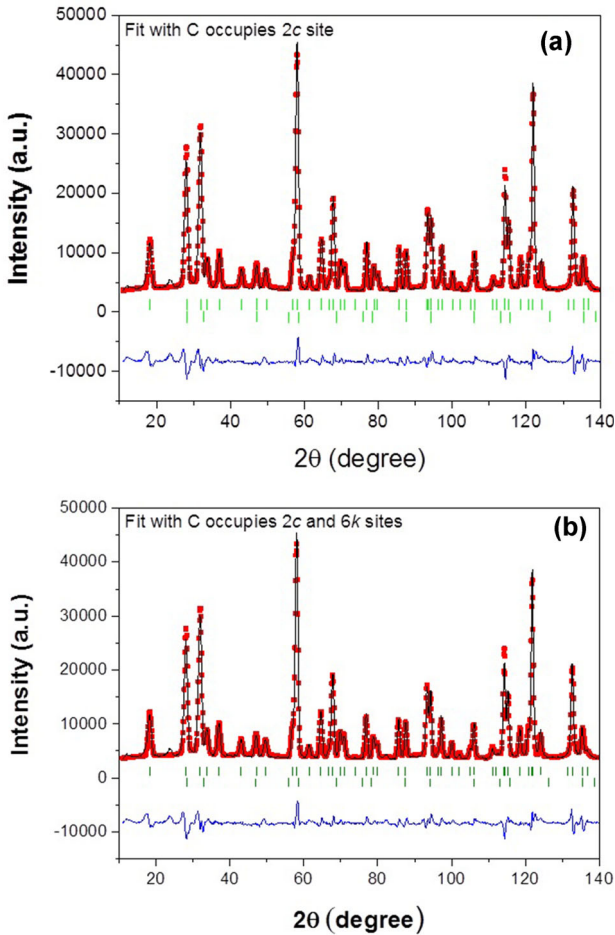Fig. 5. Powder neutron diffraction patterns for $Mn_{1.25}Fe_{0.70}P_{0.55}Si_{0.45}C_{0.025}$, fitting with carbon on the 2c site (a) and carbon on both 2c and 6k sites (b). Vertical lines indicate the Bragg peak positions for the main phase Fe_2P-type (top) and the impurity phase $(Mn,Fe)_3Si$ (bottom). Black line indicates observed profile; red squares indicate calculated data points; blue line indicates the difference between the observed and calculated profile (Color figure online).

in the parent $Mn_{1.25}Fe_{0.70}P_{0.55}Si_{0.45}$ compound. The Curie temperature of all the carbon-doped compounds is higher than that of the parent compound. Similar to the $Mn_{1.25}Fe_{0.70}P_{0.55}Si_{0.45}C_z$ series, the change in the Curie temperature of the $Mn_{1.25}Fe_{0.70}P_{0.55}Si_{0.45}C_z$ compounds does not linearly increase as a function of carbon doping concentration. It is worth mentioning that the introduction of interstitial carbon atoms in other well-known MCE materials such as $LaFe_{11.5}Si_{1.5}C_x$,[31] leads to an increase in the Curie temperature, while the Curie temperature decreases with increasing the carbon concentration for $MnAsC_x$,[32] $Ni_{43}Mn_{46}Sn_{11}C_x$,[33] and $Mn_{38}Fe_{22}Al_{40}C_x$.[34] However, no further investigation has been done on these compounds to resolve the occupancy of C in the crystal structure.

The ΔS_m of the $Mn_{1.25}Fe_{0.70}P_{0.55}Si_{0.45}C_z$ compounds in a field change of 0.5 T, 1.0 T, 1.5 T and 2.0 T derived from the isofield magnetization data is shown in Fig. 4 and summarized in Table II. As shown in Fig. 4, the ΔS_m for a field change of both 0.5 T and 1.0 T hardly changes as C is added. However, there is a slight decrease in the ΔS_m for a field change of 1.5 T and 2.0 T with carbon addition. Hence, a certain amount of C can be added to $(Mn,Fe)_2(P,Si)$ compounds in order to tune the magnetic phase transition and reduce the thermal hysteresis, while preserving an acceptable magnetocaloric effect for practical applications.

To quantify the concentration of C in the obtained samples, the combustion method using a LECO element analyzer was employed. The results obtained from the elemental analysis are in good agreement with the nominal compositions and are summarized in Table III. However, it is necessary to investigate how much and where the C atoms have entered the structure. This is not possible with x-rays as C is hardly visible for x-rays. Hence, neutron diffraction experiments were performed at room temperature to resolve the occupancy of C atoms in the crystal structure of the doped compounds.

In Fig. 5, the room-temperature neutron diffraction patterns for the $Mn_{1.25}Fe_{0.70}P_{0.55}Si_{0.45}C_z$ compounds in the paramagnetic state are shown as an example. The Rietveld refinement using the Full-Prof package for all samples confirms the Fe_2P-type hexagonal structure (space group P-62m) with two specific metallic and non-metallic sites. It is worth mentioning that <2 wt.% of the $(Mn,Fe)_3Si$ impurity phase is detected in these samples. The unit-cell volume is expected to increase if C atoms enter the structure as an interstitial element. However, the initial reduction in the unit-cell volume when carbon is added suggests that in this case C atoms substitute non-metal atoms on the 2c/1b sites, since C has a smaller atomic radius than both P and Si. Moreover, the unit-cell volume hardly changes after further C doping, indicating that part of the C added

Table IV. Structural parameters obtained from neutron diffraction data of $Mn_{1.25}Fe_{0.70}P_{0.55}Si_{0.45}C_z$ ($z = 0.000$, 0.025, 0.050, 0.075) in the paramagnetic state

	Parameters	$z = 0.000$	$z = 0.0250$	$z = 0.050$	$z = 0.075$
Unit cell	a (Å)	6.0609(1)	6.0690(1)	6.0691(1)	6.0696(1)
	c (Å)	3.4578(1)	3.4398(1)	3.4405(1)	3.4391(1)
	V (Å³)	109.996(6)	109.721(5)	109.751 (5)	109.722(5)
$3f$	x_1	0.2552(3)	0.2557(3)	0.2558(3)	0.2550(3)
	n(Fe)/n(Mn)	0.176/0.074(1)	0.181/0.069(1)	0.182/0.068(1)	0.184/0.066(1)
$3g$	x_2	0.5912(5)	0.5909(4)	0.5908(4)	0.5908(4)
	n(Mn)/n(Fe)	0.25/0.00	0.25/0.00	0.25/0.00	0.25/0.00
$2c$	n(P)/n(Si)	0.099/0.068 (2)	0.080/0.087(1)	0.078/0.089(1)	0.077/0.090(1)
	n(C)	–	0.011(1)	0.012(1)	0.014(1)
$1b$	n(P)/n(Si)	0.039/0.046(2)	0.050/0.026(1)	0.060/0.024(1)	0.061/0.023(1)
	R_p (%)	5.13	4.65	4.46	4.56
	ωR_p (%)	6.68	5.84	5.79	5.85
	χ^2	5.97	4.89	6.65	7.00

Space group: $P - 62m$. Atomic positions: $3f$ (x_1, 0, 1/2); $3g$ (x_2, 0, 1/2); $2c$ (1/3,2/3,0) and $1b$ (0,0,1/2).

Table V. Structural parameters obtained from neutron diffraction data of $Mn_{1.25}Fe_{0.70}P_{0.55}Si_{0.45}C_z$ ($z = 0.000$, 0.025, 0.050, 0.075) in the paramagnetic state

	Parameters	$z = 0.000$	$z = 0.0250$	$z = 0.050$	$z = 0.075$
Unit cell	a (Å)	6.0609(1)	6.0690(1)	6.0691(1)	6.0696(1)
	c (Å)	3.4578(1)	3.4398(1)	3.4405(1)	3.4391(1)
	V (Å³)	109.996(6)	109.722(5)	109.751 (5)	109.722(5)
$3f$	x_1	0.2552(3)	0.2555(3)	0.2556(3)	0.2560(3)
	n(Fe)/n(Mn)	0.176/0.074(1)	0.184/0.066(1)	0.185/0.065(1)	0.183/0.067(1)
$3g$	x_2	0.5912(5)	0.5910(5)	0.5911(5)	0.5915(7)
	n(Mn)/n(Fe)	0.25/0.00	0.25/0.00	0.25/0.00	0.25/0.00
$2c$	n(P)/n(Si)	0.099/0.068 (2)	0.067/0.100(4)	0.069/0.098(4)	0.079/0.088(6)
	n(C)	–	0.016(1)	0.016(1)	0.011(1)
$1b$	n(P)/n(Si)	0.039/0.046(2)	0.071/0.013(4)	0.069/0.015(4)	0.059/0.025(6)
$6k$	x_3	–	4.92(1)	4.93(1)	4.33(1)
	y_3	–	0.23(1)	0.24(2)	0.43(2)
	n(C)	–	0.07(1)	0.006(1)	0.010(1)
	R_p (%)	5.13	4.69	4.53	4.59
	ωR_p (%)	6.68	5.78	5.81	5.89
	χ^2	5.97	4.81	6.70	7.09

Space group: $P - 62m$. Atomic positions: $3f$ (x_1, 0, 1/2); $3g$ (x_2, 0, 1/2); $2c$ (1/3, 2/3, 0), $1b$ (0,0,1/2) and $6k$ (x_3, y_3, 1/2).

may also enter the interstitial sites. Hence, two different atomic models with C substituting P/Si on the $2c$ site and/or occupies the $6k$ interstitial sites have been used to resolve the occupancy of C atoms in the crystal structure. The structural parameters derived from the Rietveld refinement for the $Mn_{1.25}Fe_{0.70}P_{0.55}Si_{0.45}C_z$ compounds are summarized in Tables IV and V. It is found that in both cases the total C occupation is not strongly influenced by the amount of C added, and the Rietveld refinements are not sensitive enough to distinguish the C atom occupancy at the substitutional and/or

interstitial sites. However, the unit-cell volume decreases as C is added and hardly changes after further C doping, indicating that C atoms may enter the crystal structure both as an interstitial and a substitutional element rather than only occupy the substitutional sites. Note that Miao et al. (Ref. 23) observed an increase in the unit-cell volume as a function of the C concentration instead and pointed out that C occupies the $6k$ and $6j$ interstitial sites. This difference may come from different preparation methods since the samples of Miao and coworkers are prepared by melt spinning.

CONCLUSION

The influence of C addition on the structure and the magnetic phase transition of $Mn_{1.25}Fe_{0.70}P_{0.50}Si_{0.50}C_z$ and $Mn_{1.25}Fe_{0.70}P_{0.55}Si_{0.45}C_z$ compounds fabricated by high-energy ball milling and a solid-state reaction has been investigated. The experimental results indicate that C doping allows to tune the Curie temperature of the parent alloys and to reduce the thermal hysteresis. The magnetic softness of the C doped compounds results in large MCE even in lower magnetic fields compared to the parent compounds. The refinements based on the room-temperature neutron diffraction data indicate that C substitutes P/Si on the $2c$ site and/or occupies the $6k$ interstitial site of the hexagonal Fe_2P-type structure.

REFERENCES

1. E. Brück, *J. Phys. D Appl. Phys.* 38, R381 (2005).
2. K. Gschneidner and V. Pecharsky, *Int. J. Refrig.* 31, 945 (2008).
3. B. Yu, M. Liu, P.W. Egolf, and A. Kitanovski, *Int. J. Refrig.* 33, 1029 (2010).
4. V.K. Pecharsky and K.A. Gschneidner, *Phys. Rev. Lett.* 78, 4494 (1997).
5. H. Wada and Y. Tanabe, *Appl. Phys. Lett.* 793302 (2001).
6. H. Wada, T. Morikawa, K. Taniguchi, T. Shibata, Y. Yamada, and Y. Akishige, *Phys. B: Condens. Matter* 328, 114 (2003).
7. O. Tegus, E. Brück, K.H.J. Buschow, and F.R. de Boer, *Nature* 415, 150 (2002).
8. N.T. Trung, Z.Q. Ou, T.J. Gortenmulder, O. Tegus, K.H.J. Buschow, and E. Brück, *Appl. Phys. Lett.* 4, 102513 (2009).
9. D.T. Cam Thanh, E. Brück, N.T. Trung, J.C.P. Klaasse, K.H.J. Buschow, Z.Q. Ou, O. Tegus, L. Caron, and L. Caron, *J. Appl. Phys.* 103, 07B318 (2008).
10. F. Guillou, H. Yibole, G. Porcari, L. Zhang, N.H. van Dijk, and E. Brück, *J. Appl. Phys.* 116, 063903 (2014).
11. N. Trung, L. Zhang, L. Caron, K. Buschow, and E. Brück, *Appl. Phys. Lett.* 96, 172504 (2010).
12. D. Zhang, Z. Nie, Z. Wang, L. Huang, Q. Zhang, and Y.D. Wang, *J. Magn. Magn. Mater.* 387, 107 (2015).
13. J. Chen, Z. Wei, E. Liu, X. Qi, W. Wang, and G. Wu, *J. Magn. Magn. Mater.* 387, 159 (2015).
14. F.X. Hu, M. Ilyn, A.M. Tishin, J.R. Sun, G.J. Wang, Y.F. Chen, F. Wang, Z.H. Cheng, and B.G. Shen, *J. Appl. Phys.* 93, 5503 (2003).
15. A. Fujita, S. Fujieda, Y. Hasegawa, and K. Fukamichi, *Phys. Rev. B* 67, 104416 (2003).
16. A. Barcza, M. Katter, V. Zellmann, S. Russek, S. Jacobs, and C. Zimm, *IEEE Trans. Magn.* 47, 3391 (2011).
17. M.P. Annaorazov, K.A. Asatryan, G. Myalikgulyev, S.A. Nikitin, A.M. Tishin, and A.L. Tyurin, *Renew. Sustain. Energy Rev.* 32, 867 (1992).
18. F. Hu, B. Shen, J. Sun, and G. Wu, *Phys. Rev. B* 64, 132412 (2001).
19. J. Liu, T. Gottschall, K.P. Skokov, J.D. Moore, and O. Gutfleisch, *Nat. Mater.* 11, 620 (2012).
20. X.F. Miao, L. Caron, P. Roy, N.H. Dung, L. Zhang, W.A. Kockelmann, R.A. de Groot, N.H. van Dijk, and E. Brück, *Phys. Rev. B* 89, 174429 (2014).
21. N.H. Dung, Z.Q. Ou, L. Caron, L. Zhang, D.T.C. Thanh, G.A. De Wijs, R.A. De Groot, K.H.J. Buschow, and E. Brück, *Adv. Energy Mater.* 1, 1215 (2011).
22. N.V. Thang, X.F. Miao, N. van Dijk, and E. Brück, *J. Alloys Compd.* 670, 123 (2016).
23. X.F. Miao, N.V. Thang, L. Caron, H. Yibole, R.I. Smith, N.H. van Dijk, and E. Brück, *Scr. Mater.* 124, 129 (2016).
24. N.V. Thang, H. Yibole, N. van Dijk, and E. Brück, *J. Alloys Compd.* 699, 633 (2017).
25. N.V. Thang, N. Dijk, and E. Brück, *Materials* 10, 14 (2017).
26. N.H. Dung, L. Zhang, Z.Q. Ou, L. Zhao, L. van Eijck, A.M. Mulders, M. Avdeev, E. Suard, N.H. van Dijk, and E. Brück, *Phys. Rev. B* 86, 045134 (2012).
27. L. van Eijck, L.D. Cussen, G.J. Sykora, E.M. Schooneveld, N.J. Rhodes, A. van Well, and C. Pappas, *J. App. Crystallogr.* 49, 1 (2016).
28. J. Rodríguez-Carvajal, *Phys. B: Condens. Matter* 192, 55 (1993).
29. X.F. Miao, L. Caron, Z. Gercsi, A. Daoud-Aladine, N.H. van Dijk, and E. Brück, *Appl. Phys. Lett.* 107, 042403 (2015).
30. F. Guillou, H. Yibole, N. van Dijk, and E. Brück, *J. Alloys Compd.* 632, 717 (2015).
31. S. Li, R. Huang, Y. Zhao, W. Wang, and L. Li, *Phys. Chem. Chem. Phys.* 17, 30999 (2015).
32. W.B. Cui, W. Liu, Q. Zhang, B. Li, X.H. Liu, F. Yang, X.G. Zhao, and Z.D. Zhang, *J. Magn. Magn. Mater.* 322, 2223 (2010).
33. Y. Zhang, J. Liu, Q. Zheng, J. Zhang, W. Xia, J. Du, and A. Yan, *Scr. Mater.* 75, 26 (2014).
34. Q. Guo, Z. Ou, R. Han, W. Wei, S. Ebisu, and O. Tegus, *Chem. Phys. Lett.* 640, 137 (2015).